

Supplementary Material

Supplementary Methods

Animal studies

24 hour urine samples, to assess albumin (mouse albumin ELISA-kit, Bethyl Laboratories) and creatinine (Sentinel Kit, Sentinel, Milan, Italy) values, were obtained by placing the animals in metabolic cages. These measurements allowed calculation of UAlb/UCreat, which is a better measure of glomerular permeability than urinary albumin alone, especially in mice.

To collect renal tissue, animals were sacrificed either by decapitation, or anaesthetized by clorarium hydrate and perfused by cold PBS. In both cases, kidneys were taken and material for routine light microscopy stainings was fixed in 4% buffered paraformaldehyde, dehydrated, and paraffin-embedded. For transmission electron microscopy, 1mm³ renal cortex pieces were fixed in a mixture of paraformaldehyde, glutaraldehyde, and phosphate buffer, and embedded in resin. For scanning electron microscopy, pieces of cortex were fixed in a mixture of glutaraldehyde 2% and paraformaldehyde 4% in phosphate buffer 0,12 M for 6 h, fixed in a mixture of osmium tetroxide 1% and sodium cacodylate buffer 0,12M for 2 h, dehydrated in a graded ethanol series and dried in hexamethyldisilazane (all reagents from Electron Microscopy Sciences, Società Italiana Chimici, Roma, Italy). Then the pieces were sputter-coated with gold (Edwards S150A sputter coater). For immunofluorescence, the unfixed renal tissue was embedded in OCT (optimum cutting temperature cryoembedding matrix) (Tissue-Tek, Electron Microscopy Sciences), snap-frozen in a mixture of isopentane and dry ice, and stored at -80°C. For immunogold electron microscopy on ultracryosections, tissue was fixed in a mixture of paraformaldehyde, glutaraldehyde, and phosphate buffer, soaked in saccarose 18% and frozen on the top of specimen pins (Electron Microscopy Sciences).

Immunofluorescence studies

Apart from F-actin, directly detected by Phalloidin-TRITC (Sigma-Aldrich), an indirect immunofluorescence method was applied on 5µm-thick acetone-fixed tissue cryosections and on acetone-fixed cultured cells.

The following primary antibodies were used for the study: rabbit anti-mouse nephrin (intracellular domain) (#035, provided by H. Holthofer, Dublin City University, Ireland), mouse anti-synaptopodin (Progen, Heidelberg, Germany), rabbit anti-podocin (Sigma-Aldrich), rabbit anti-WT1 (C-19) (Santa Cruz Biotechnology, Santa Cruz, CA, USA), rabbit anti-ZO-1 (Invitrogen, S.

Giuliano Milanese, Italy), rabbit anti-alpha-actinin-4 (LifeSpan Biosciences, Seattle, WA, USA), mouse anti-smooth muscle actin alpha isoform (α -SMA, Invitrogen), rat anti-mouse CD31/PECAM (Abcam, Cambridge, UK), mouse anti-pan cytokeratin (Abcam), rabbit anti-non muscle myosin IIA (Abcam), rabbit anti-NMDA1 receptor (Abcam), mouse anti-Rab3A (Synaptic System), rabbit anti-rabphilin-3A (BD Transduction Laboratories, Milan, Italy), rabbit anti-Synapsin-I (Sigma-Aldrich), rabbit anti-phospho-(S603)-Synapsin-I (Sigma-Aldrich), rabbit anti-CaMKII (Abcam), rabbit anti-phospho-(T286)-CaMKII (Abcam), rabbit anti-cofilin (Abcam), rabbit anti phospho-(S3)-cofilin (Abcam), rabbit anti-alpha-tubulin (Abcam).

As secondary fluorescent-labelled antibodies, we used the following: Alexa Fluor 488 (or 546) goat anti-rabbit IgG, Alexa Fluor 488 (or 546) goat anti-mouse IgG highly cross adsorbed, and Alexa Fluor 488 chicken anti-rat IgG highly cross adsorbed (all from Invitrogen).

Specificity of Ab labelling was demonstrated by the lack of staining after substituting proper control immunoglobulins (rabbit primary Ab isotype control and mouse primary Ab isotype control, both from Invitrogen, and Rat IgG1 negative control, from Serotec, Kidlington Oxford, UK) for the primary antibodies.

Slides were mounted with VectaShield aqueous mounting medium (Vector Laboratories, DBA Italia SRL, Milan, Italy).

Images were acquired by a Zeiss AxioScope 40FL microscope, equipped with AxioCam MRc5 digital videocamera and immunofluorescence apparatus (Carl Zeiss SpA), and recorded by AxioVision software 4.3.

Western Blot

Glomeruli and cells were lysed in RIPA buffer, protein lysates were separated on a SDS-PAGE and transferred by electroblotting on a PVDF membrane (ImmunBlot PVDF membrane, BioRad Laboratories Inc., CA, USA). After blocking, each membrane was incubated with the primary antibody, followed by the proper HRP (horseradish peroxidase)-conjugated secondary antibody, and positive reaction products were identified by chemiluminescence (BM Chemiluminescence Western Blotting Kit, Roche). Images were digitally acquired by Chemidoc XRS instrument (Bio-Rad, Milan, Italy).

Supplementary Figure legends

Suppl.Fig 1. In situ hybridization

In situ hybridization demonstrates synthesis of Rab3A and NMDAR1 in glomeruli from a 3 month old Balb/c mouse (left panels), and negative controls (right panels) obtained by sense probes (630X, scale bars 20µm).

In situ hybridization was performed as described.^{suppl.Ref1} Briefly, tissues were deparaffinized and rehydrated, then permeabilized and post-fixed. Sections were then acetylated by acetic-anhydride/trietanolamine, washed, and incubated with prehybridization solution. Biotin-labelled probes were applied overnight in a water-saturated atmosphere. The following probes were used: Rab3A antisense: GCA TAG ACT TCA AGG TCA AAA CCA TCT ACC GCA ACG ACA AGA GGA TCA AGC TGC AGA TCT; Rab3A sense: AGA TCT GCA GCT TGA TCC TCT TGT CGT TGC GGT AGA TGG TTT TGA CCT TGA AGT CTA TGC.

Considering that the NMDAR1 subunit has eight splicing variants, we used the same probes as Laurie et al,^{suppl.Ref2} specifically designed to span all subunits and detect total NMDAR1 mRNA: NMDAR1 antisense: GCT CTT GGA AGA TAC AGC TCA ACG CCA CTT CTG TCA CCC ACA AGC; NMDAR1 sense: GCT TGT GGG TGA CAG AAG TGG CGT TGA GCT GTA TCT TCC AAG AGC.

After hybridization, stringency washes were performed with SSC (standard sodium citrate) 4X, SSC 2X-50% formamide at 45°C, and again with SSC 1X at room temperature. Specimens were then incubated with alkaline phosphatase-labelled streptavidin and the reaction developed with Fast Red (all reagents from Sigma, nucleotides from Eurofins MWG Operon, Ebersberg, Germany).

Suppl.Fig 2. Double stainings

Fig 2A: Double staining immunofluorescence reveals glomerular areas co-stained by Rab3A (in red) and podocin (green), as shown by the yellow labelling on the merge picture (400X, scale bars 50µm).

Fig 2B: Podocin (green) and rabphilin-3A (red) co-labelling is revealed by the yellow glomerular staining after image merging (400X, scale bars 50µm).

Double staining was obtained by repeating twice the indirect immunofluorescence procedure described in the Concise Methods.

Suppl.Fig 3. Podocyte foot process effacement

Both images (scale bars 1 μ m) from a Rab3A-KO mouse clearly show areas of foot process effacement.

Suppl.Fig 4. Three month old Rab3A-KO and WT mice: immunofluorescence analysis of podocyte proteins.

Immunofluorescence demonstrates segmental loss of the podocyte markers nephrin (4A), podocin (4B), synaptopodin (4C), alpha-actinin4 (4D), and ZO-1 (4E), indicated by white arrows, in glomeruli of 3 month old Rab3A-KO mice (upper panels) and absent from glomeruli of corresponding WT animals (lower panels) (all images 400X, scale bars 50 μ m, but WT-synaptopodin in Fig 4C, taken at 200X, scale bar 100 μ m).

Quantification of data, obtained from 5 mice per strain and 30 glomeruli per specimen, is represented in Fig 4F, where podocyte markers have been evaluated either as percentage of the glomerular area occupied by the staining, and as percentage of glomeruli with segmental loss of staining.

These alterations were not accompanied by variations of podocyte number in KO glomeruli compared to the WT, as shown by Fig 4G, where the graph summarizes the quantitative data obtained from calculation of the number of WT-1 positive cells per glomerulus (representative immunofluorescence, lower panel, 400X, scale bars 50 μ m) in 3 mice per strain and 30 glomeruli per tissue.

Quantitative evaluations were performed on digitalized images by using appropriate macros (essentially formed by color threshold procedure and filtering) applied on glomerular areas selected as region of interests (ROI). The software (AxioVision 4.7 Quantification Modules, Zeiss) was programmed to automatically calculate percentages of the area or number of particles per ROI, according to the specific needs.

Suppl.Fig 5. Immunogold electron microscopy

Fig 5A: In a WT mouse glomerulus, Synapsin-1, detected by immunogold electron microscopy (upper panel, scale bar 200nm), displays several dots of positivity in the foot processes, as indicated by the red arrows, whereas phospho-Synapsin-1 (lower panel, scale bar 500nm) can not be detected (scale bar 200nm).

Fig 5B: Only a single dot of Synapsin-I positivity (upper panel, scale bar 200nm) can be observed in this tissue from a KO animal, whereas phospho-Synapsin-I appears relatively more represented (lower panel, scale bar 200nm), as evidenced in both figures by the red arrows.

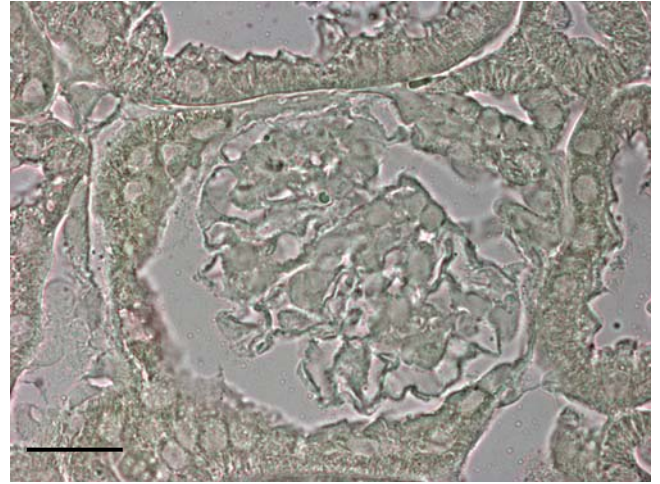
Supplementary References

1. Rastaldi MP, Ferrario F, Giardino L, Dell'Antonio G, Grillo C, Grillo P, Strutz F, Müller GA, Colasanti G, D'Amico G: Epithelial-mesenchymal transition of tubular epithelial cells in human renal biopsies. *Kidney Int* 62: 137-146, 2002
2. Laurie DG, Seeburg PH: Regional and developmental heterogeneity in splicing of the rat brain NMDAR1 mRNA. *J Neurosci* 14: 3180-3194, 1994

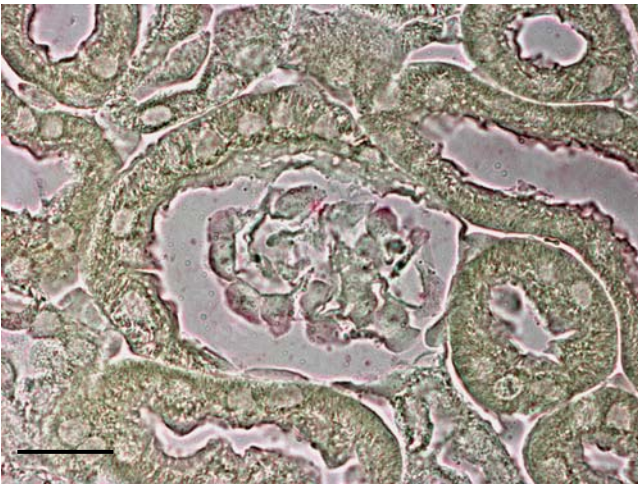
Rab3A – antisense probe



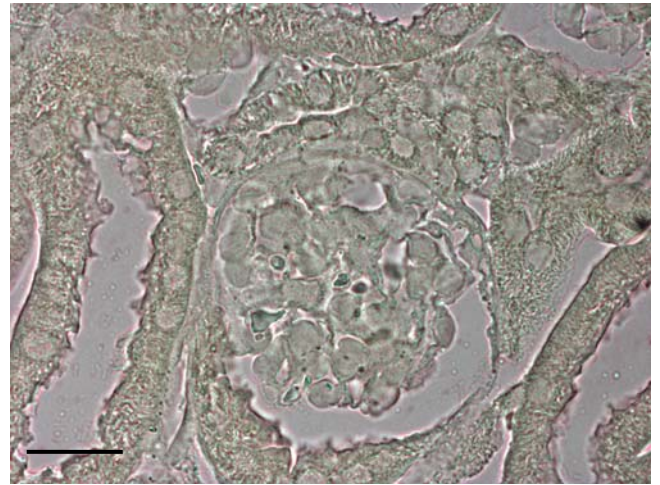
Rab3A – sense probe



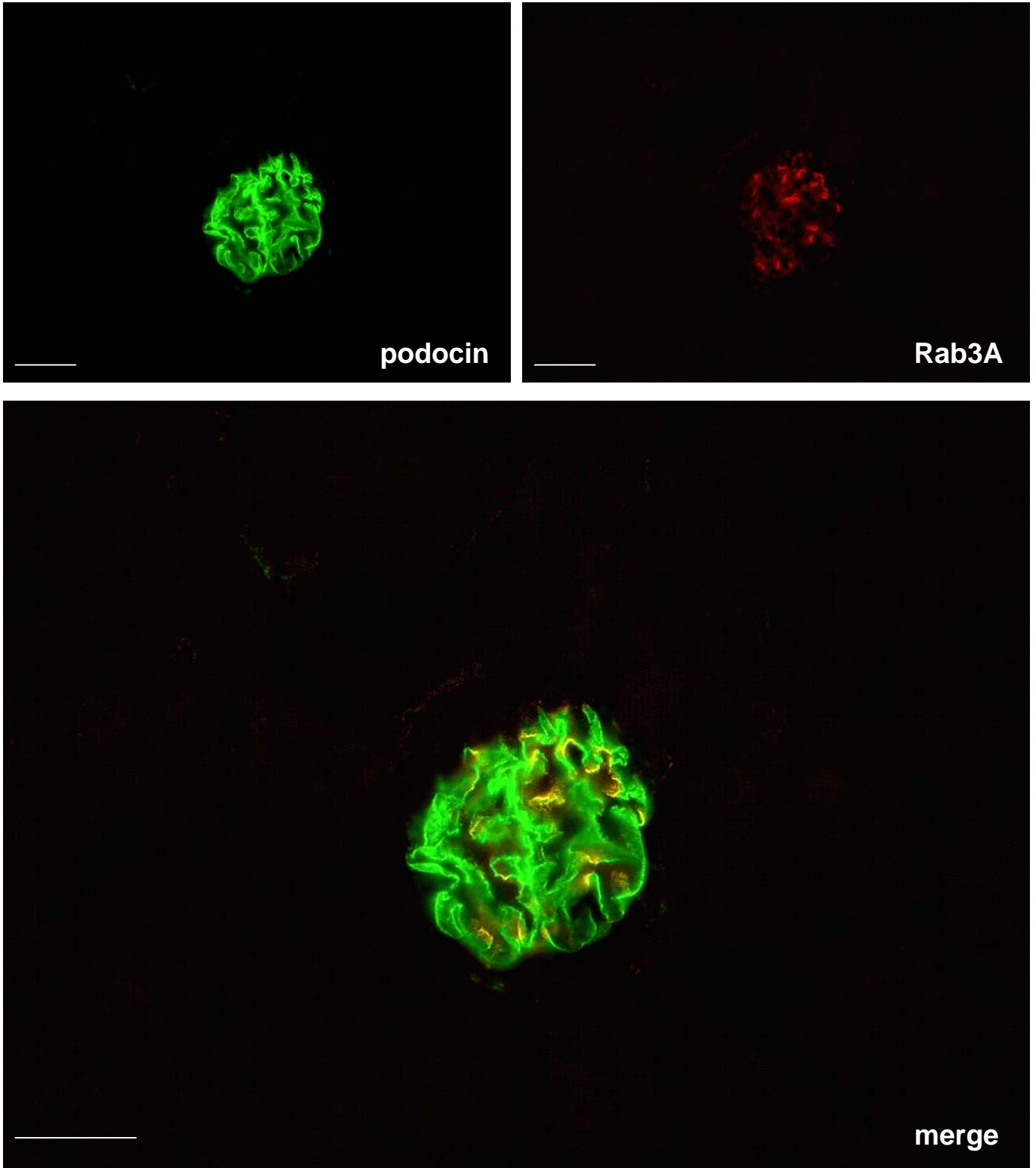
NMDAR1 – antisense probe



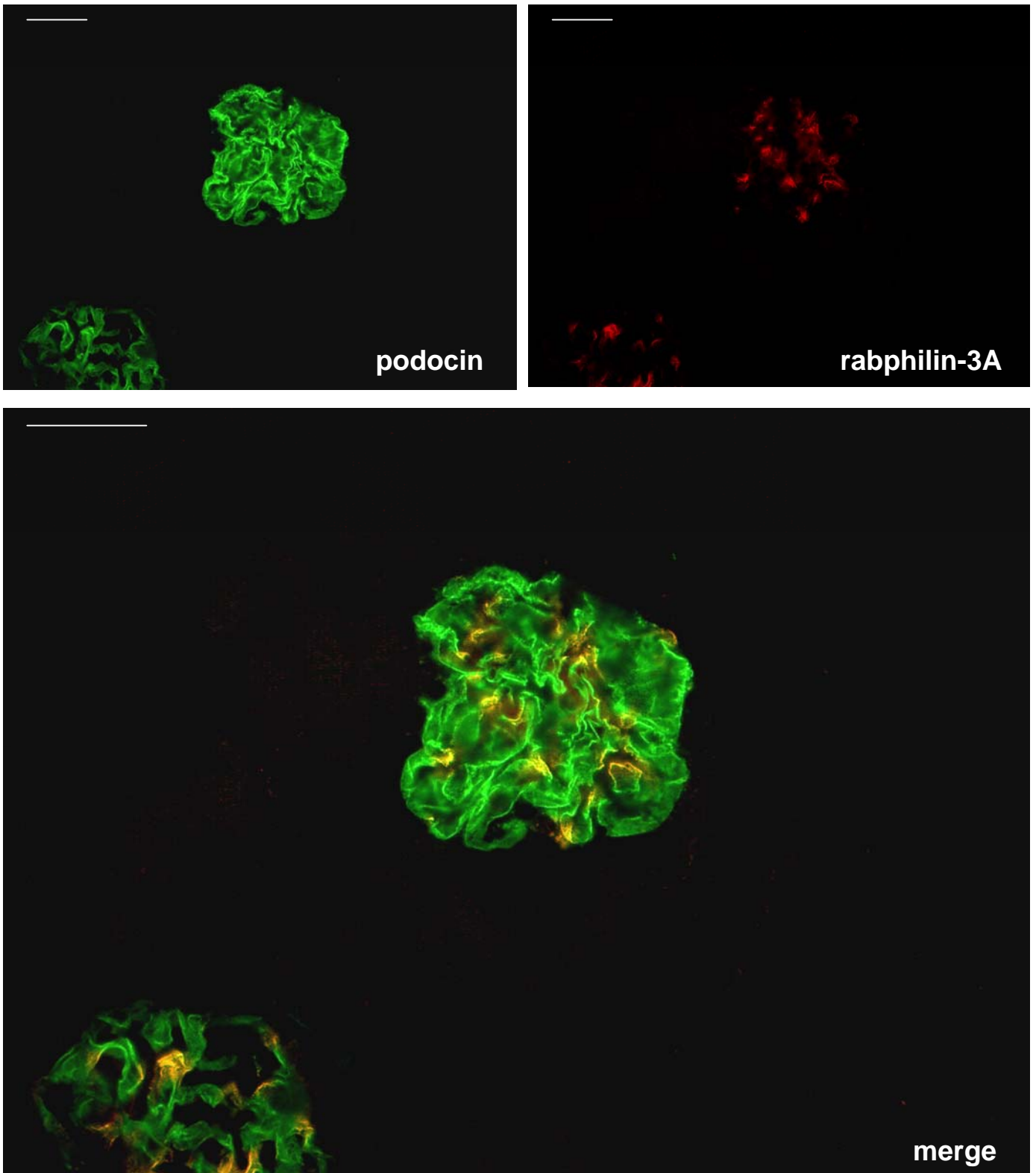
NMDAR1 – sense probe



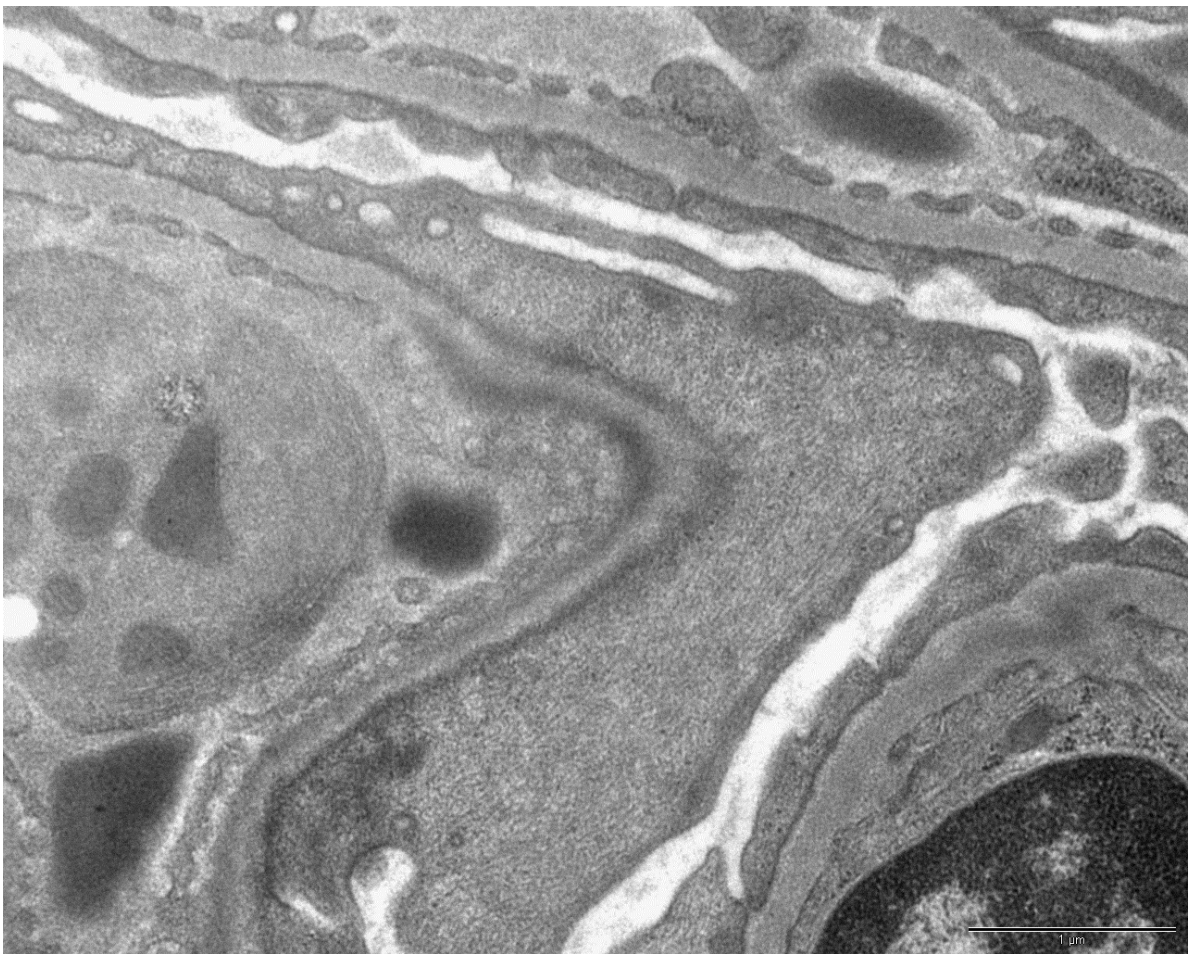
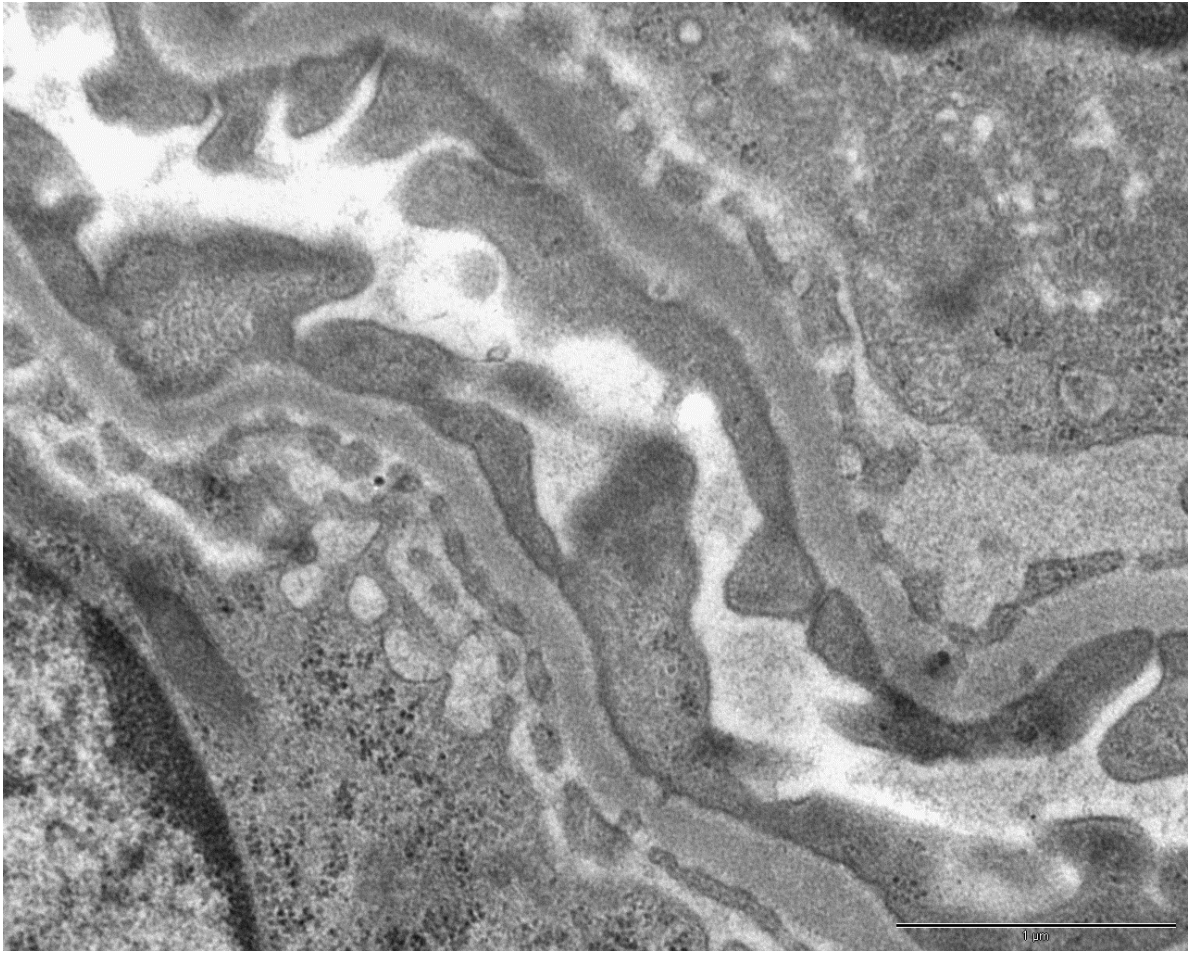
Suppl.Fig 1



Suppl.Fig 2A

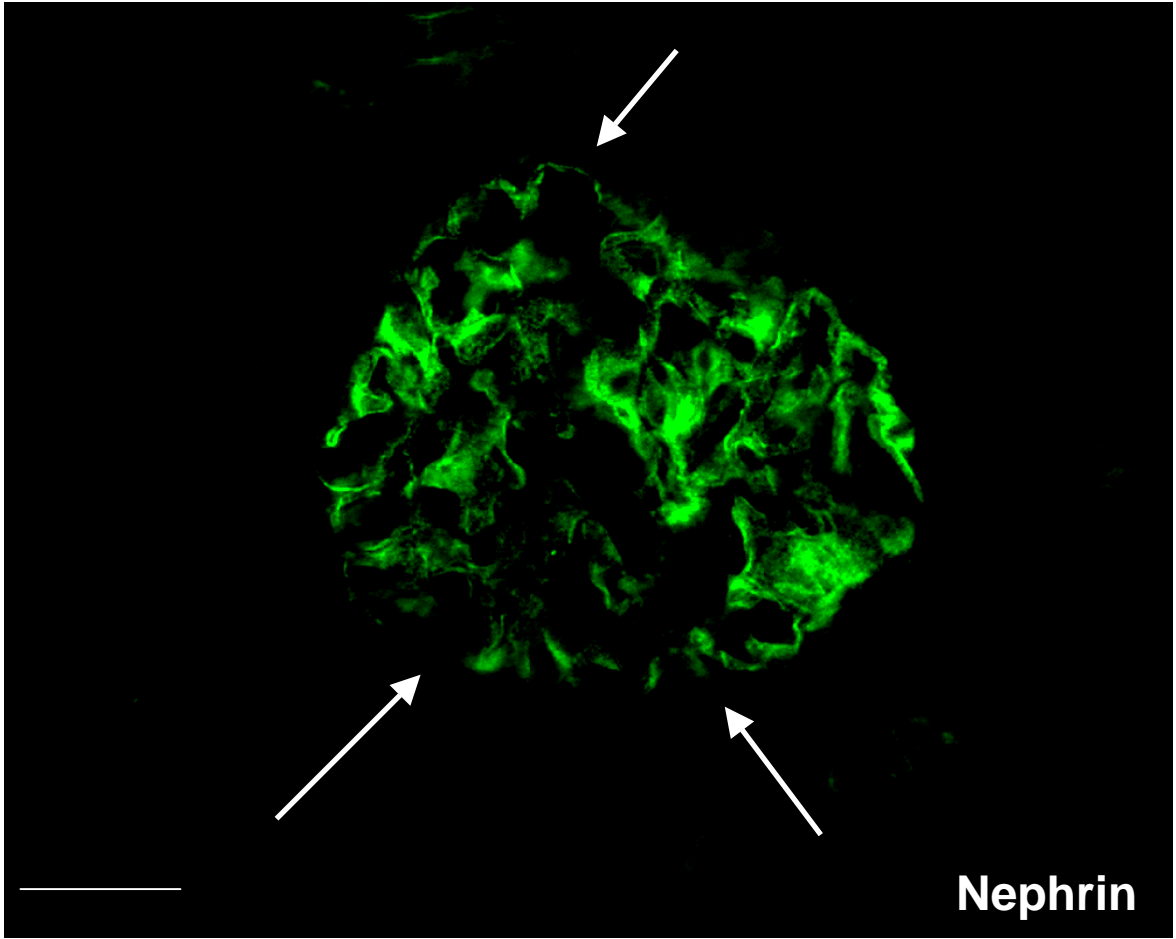


Suppl.Fig 2B

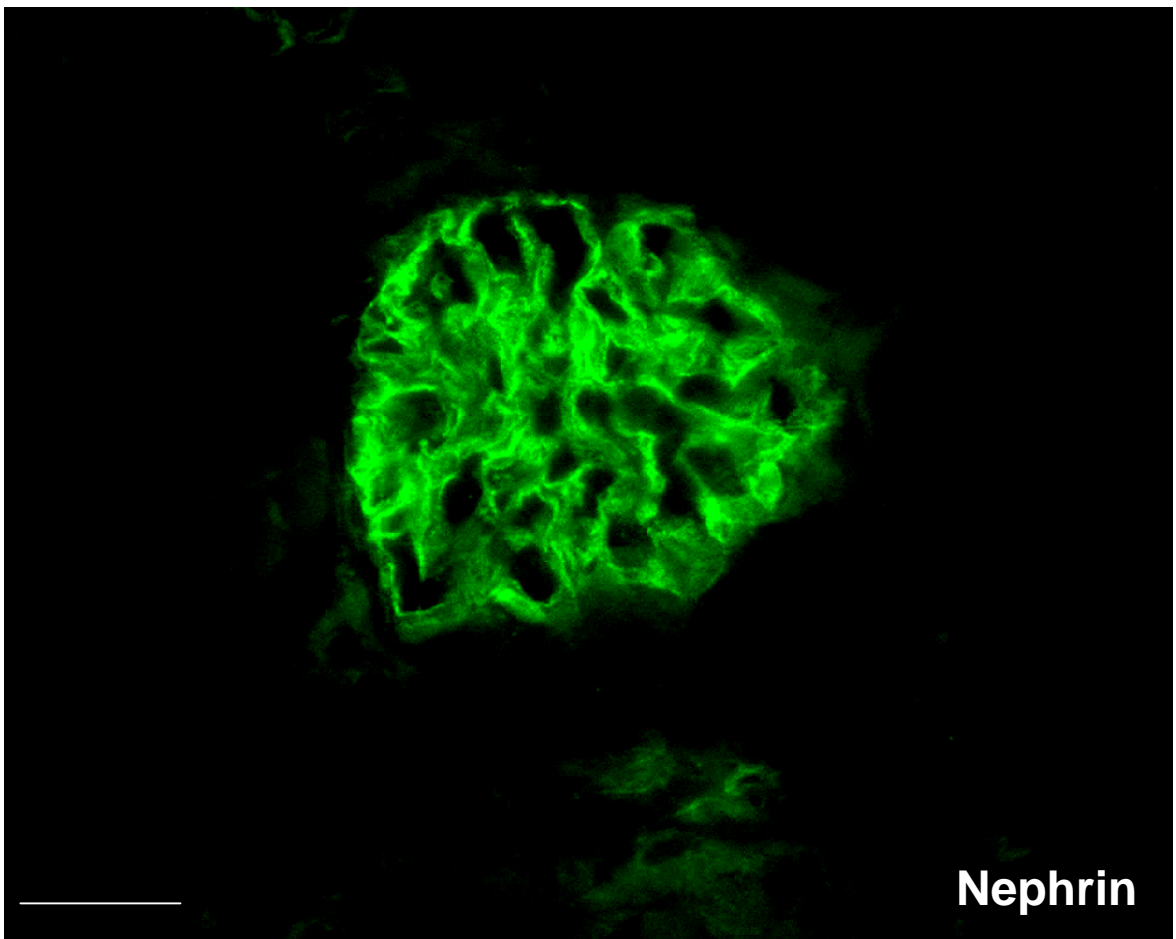


Suppl.Fig 3

KO

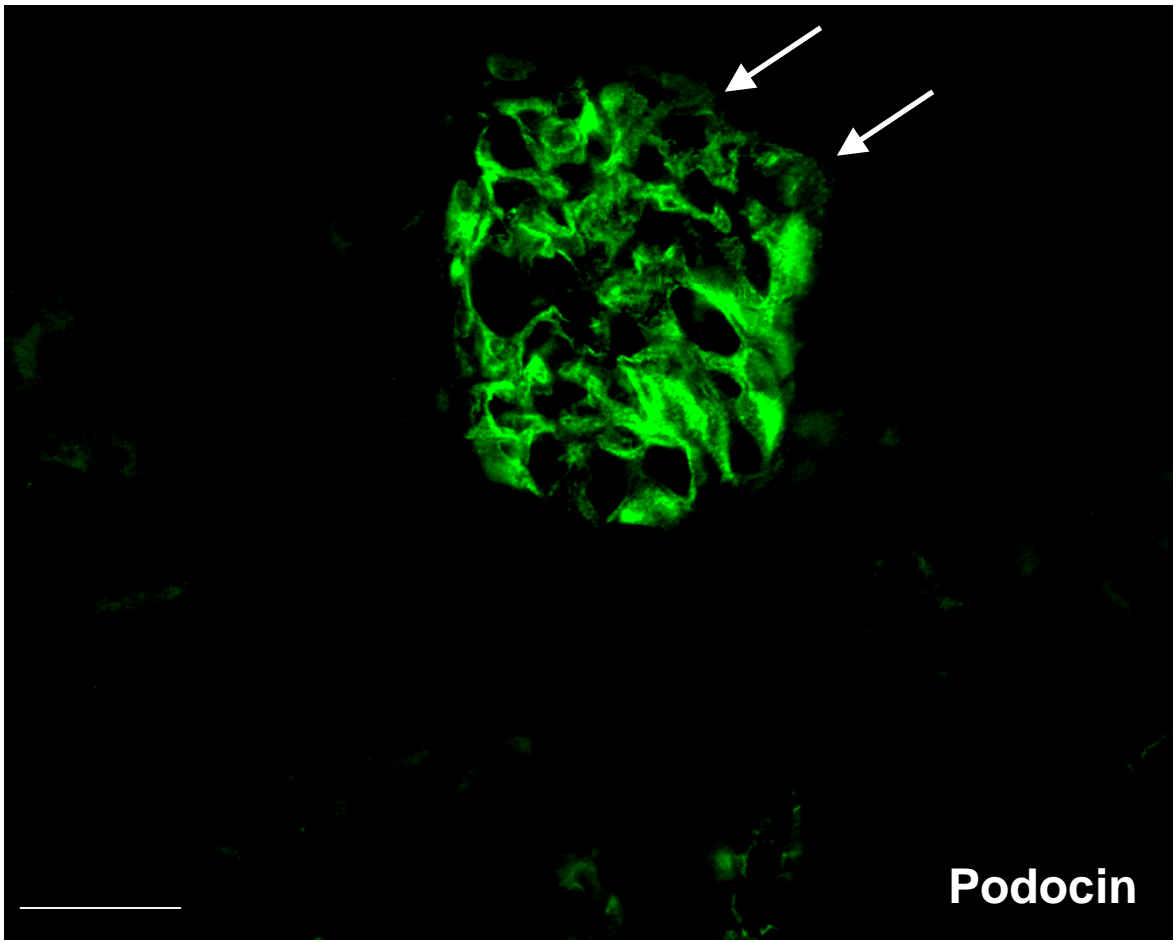


WT

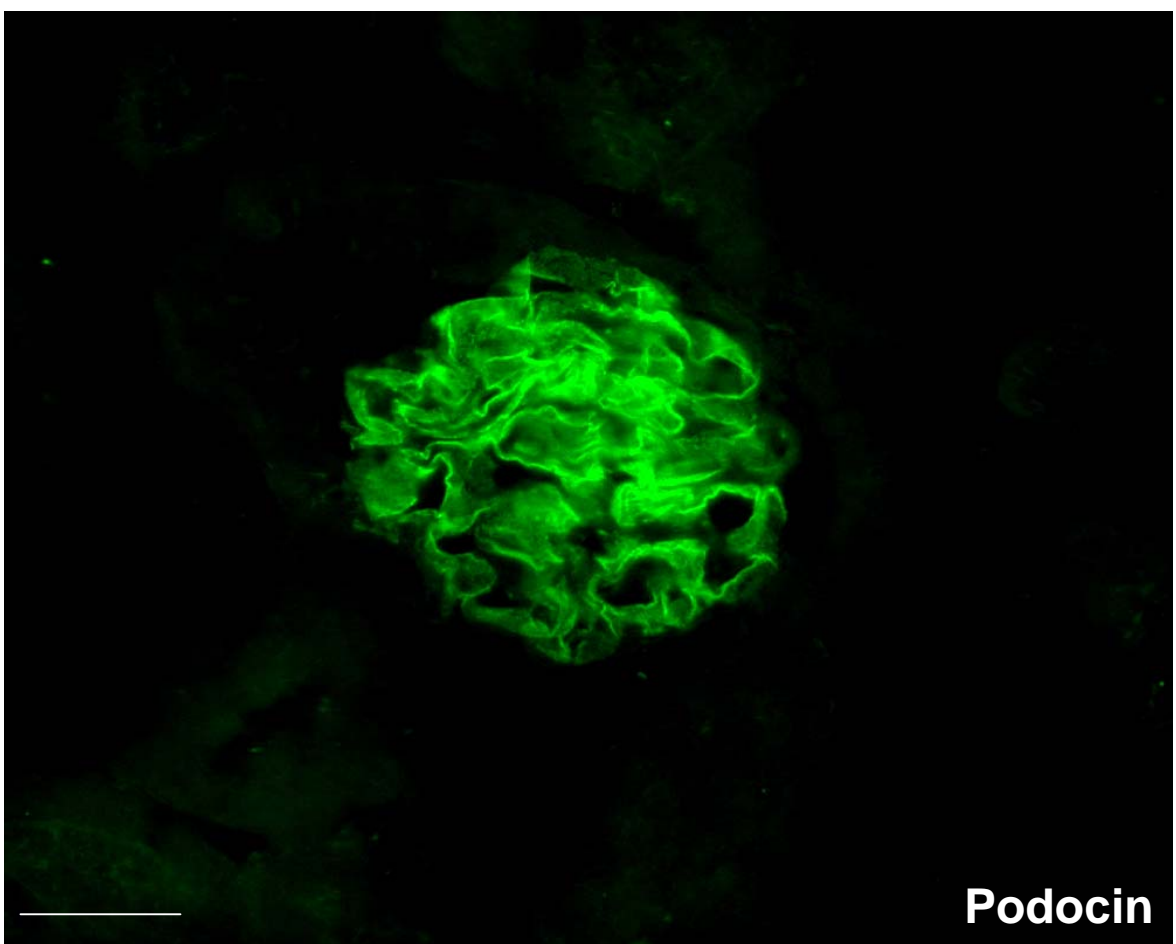


Suppl.Fig 4A

KO

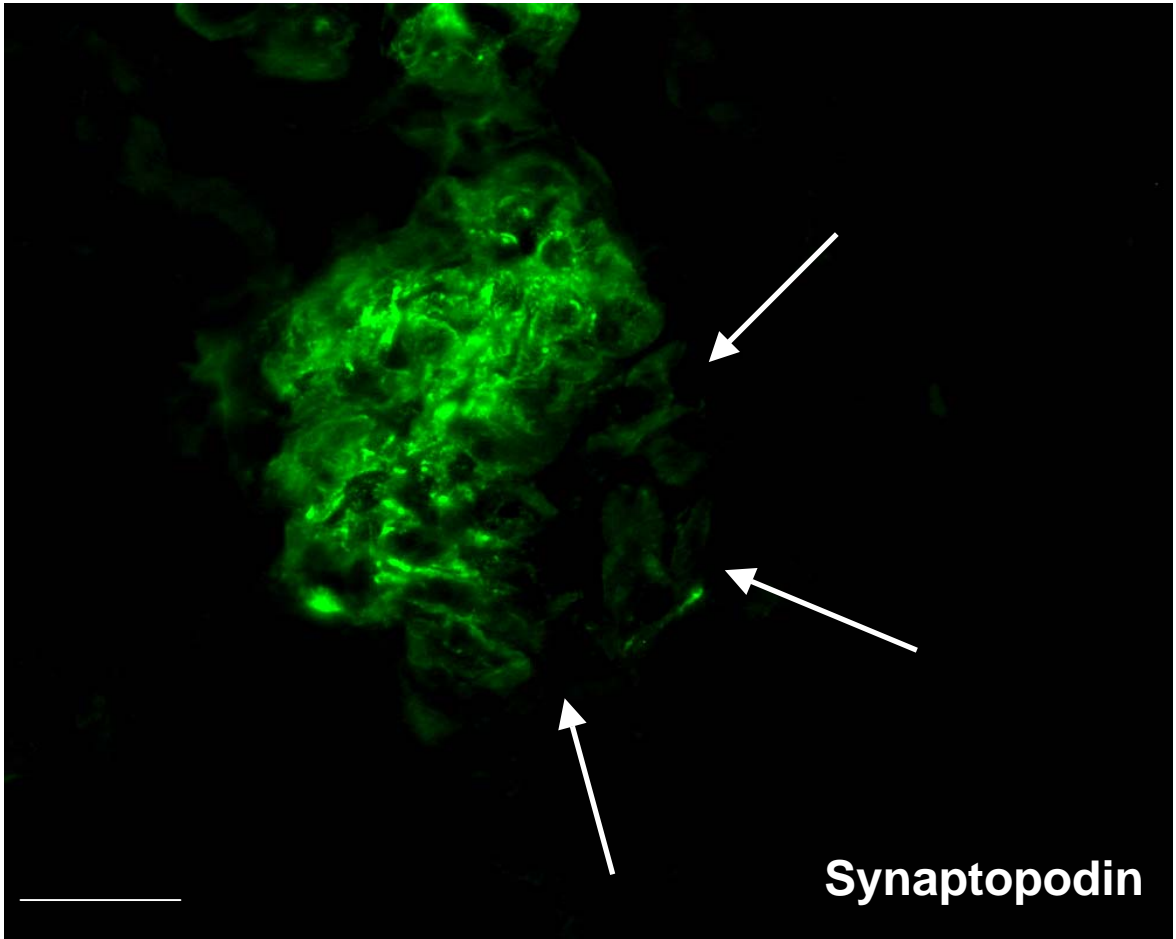


WT

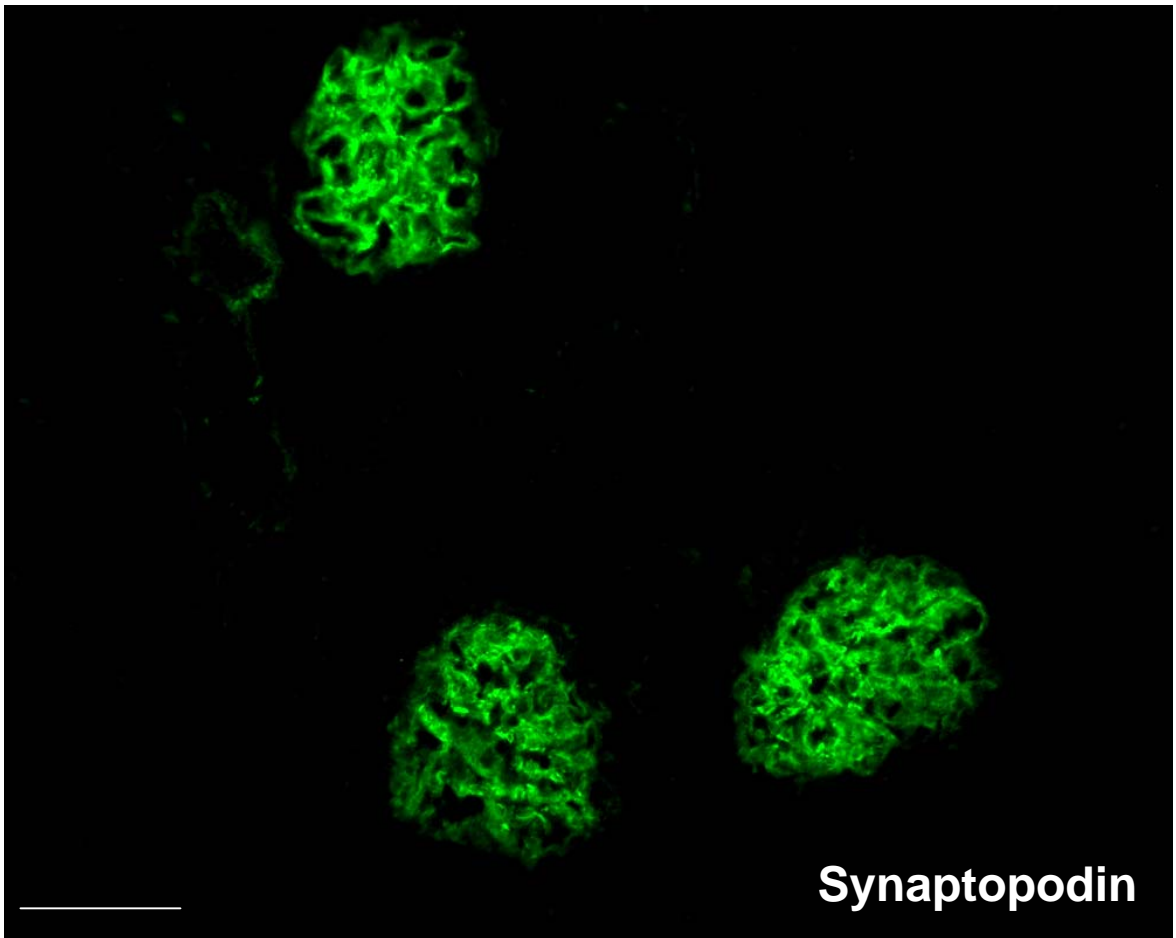


Suppl.Fig 4B

KO

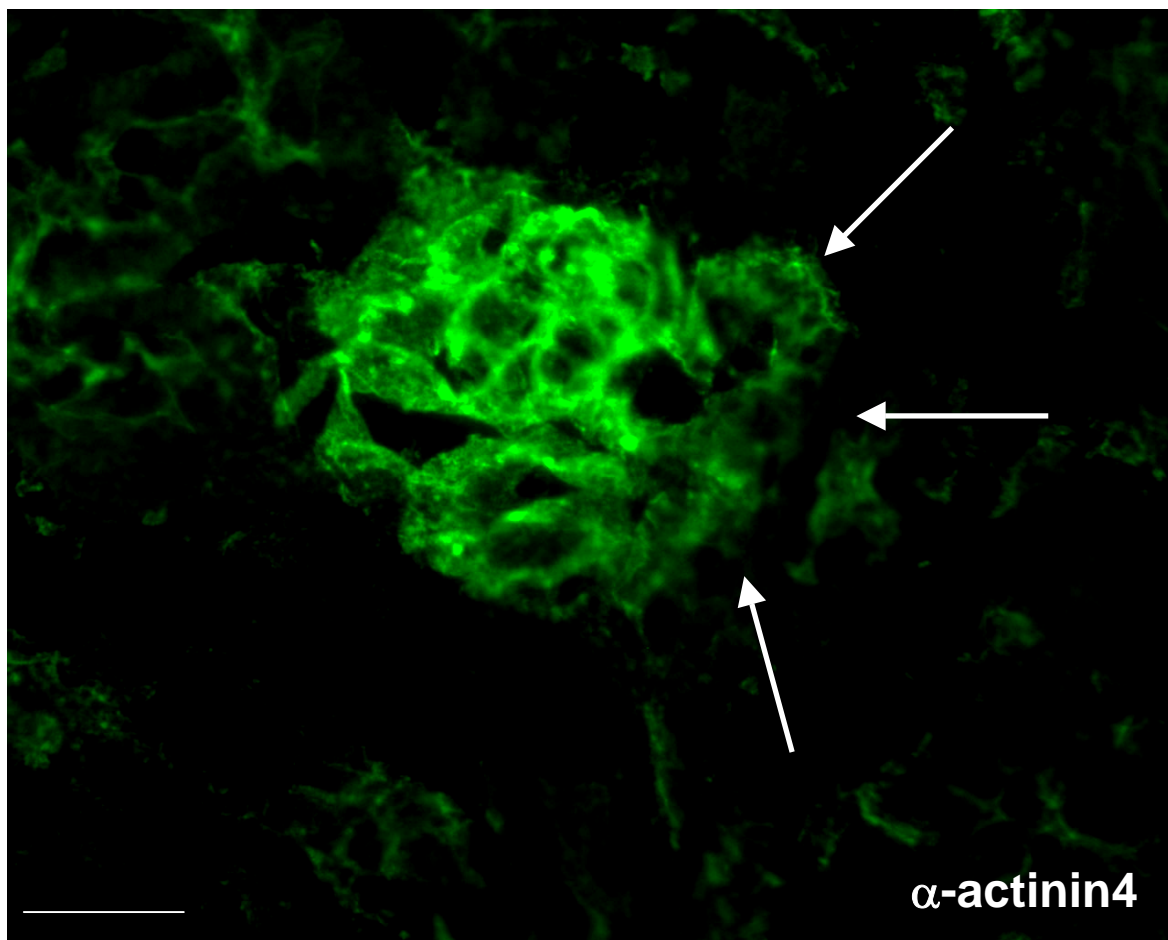


WT

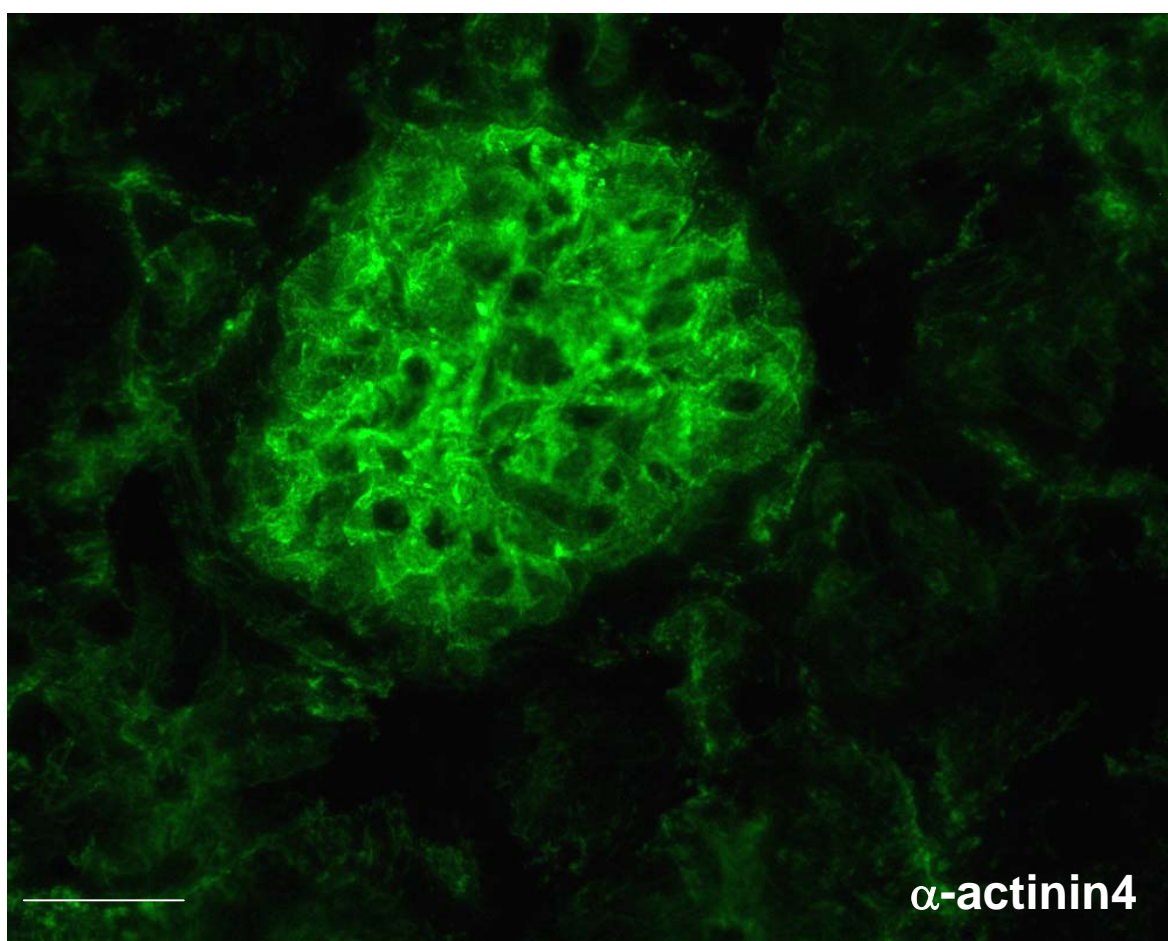


Suppl.Fig 4C

KO

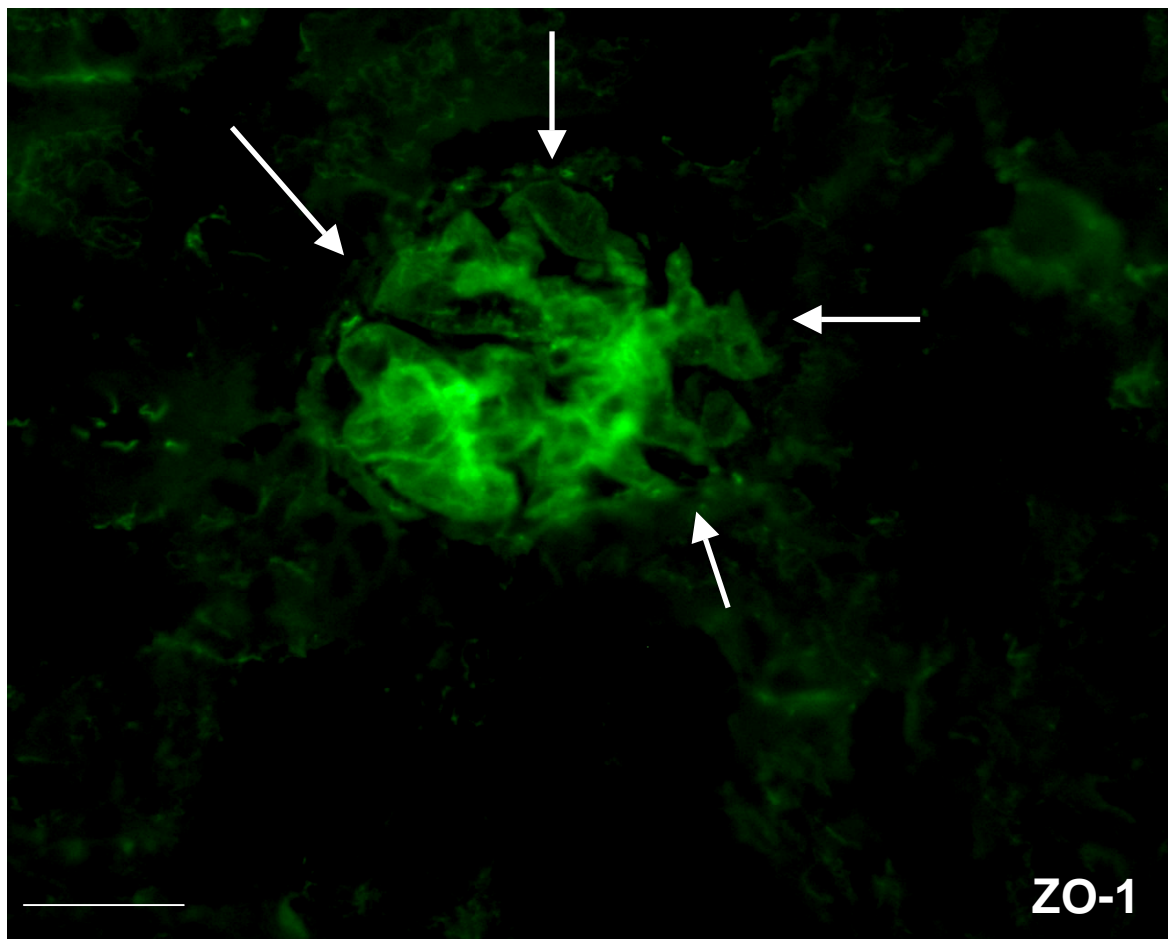


WT

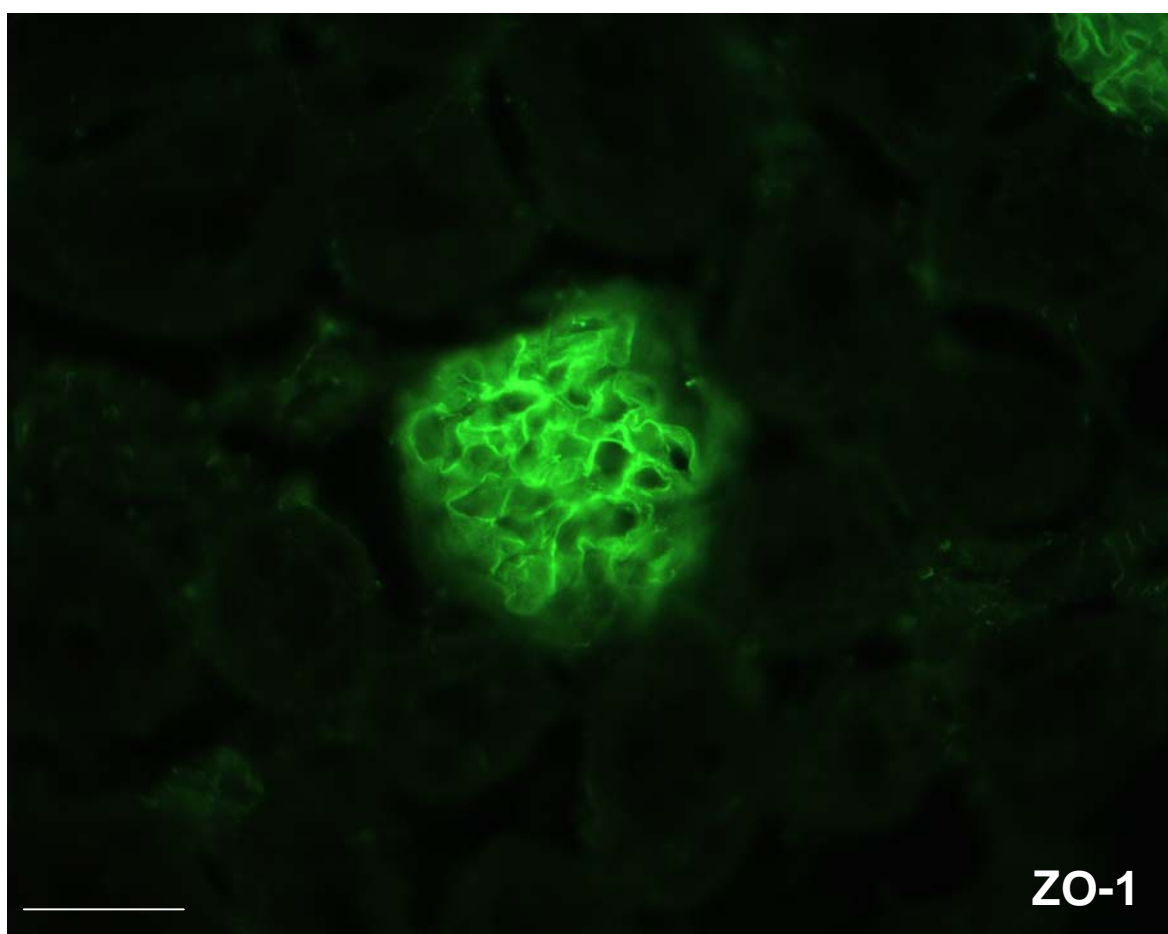


Suppl.Fig 4D

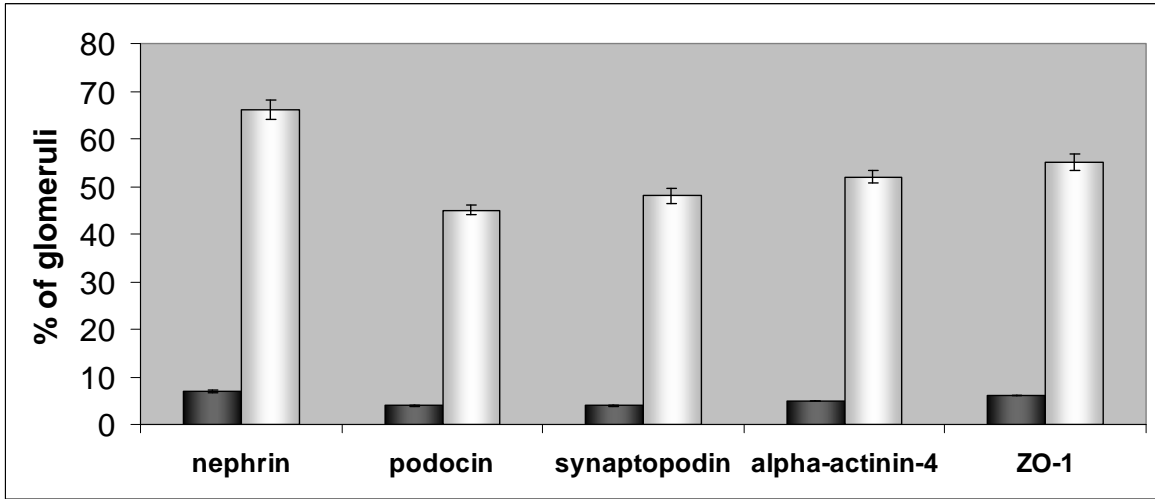
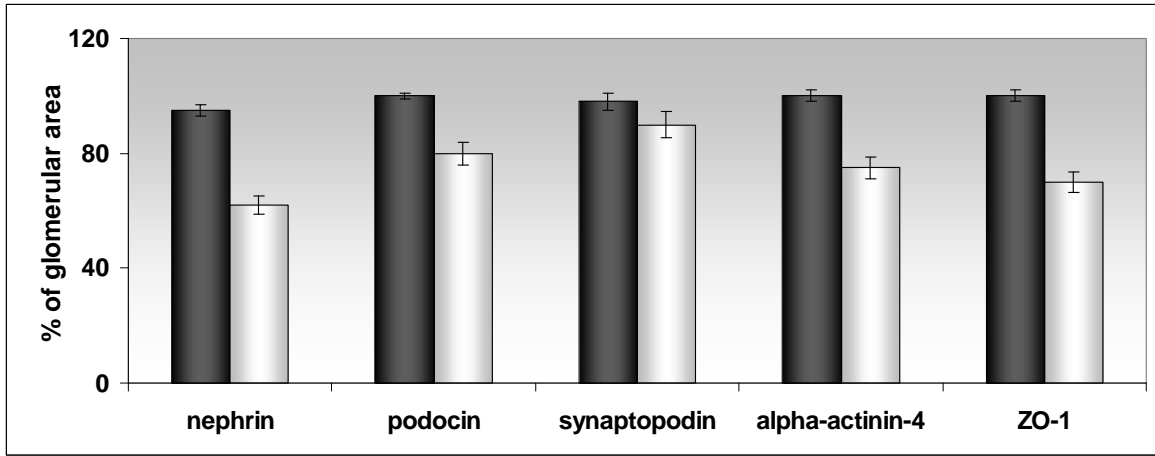
KO



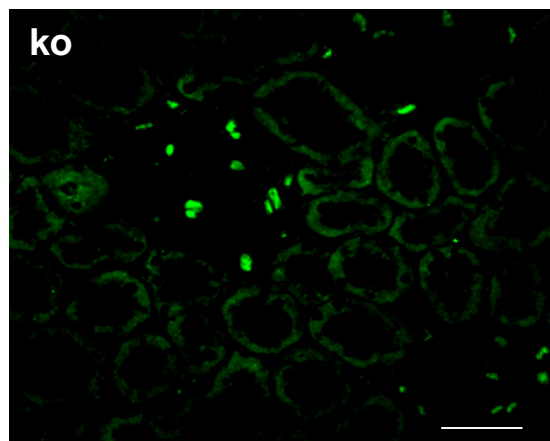
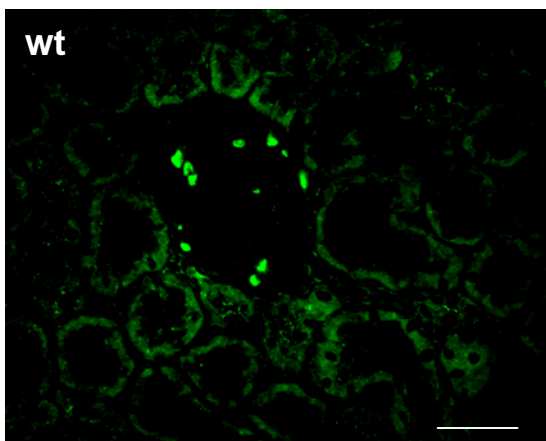
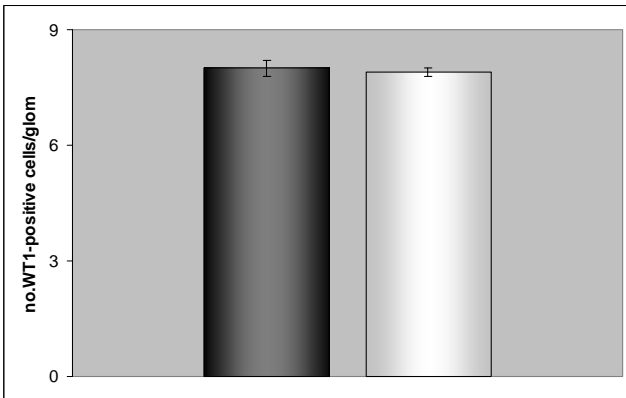
WT



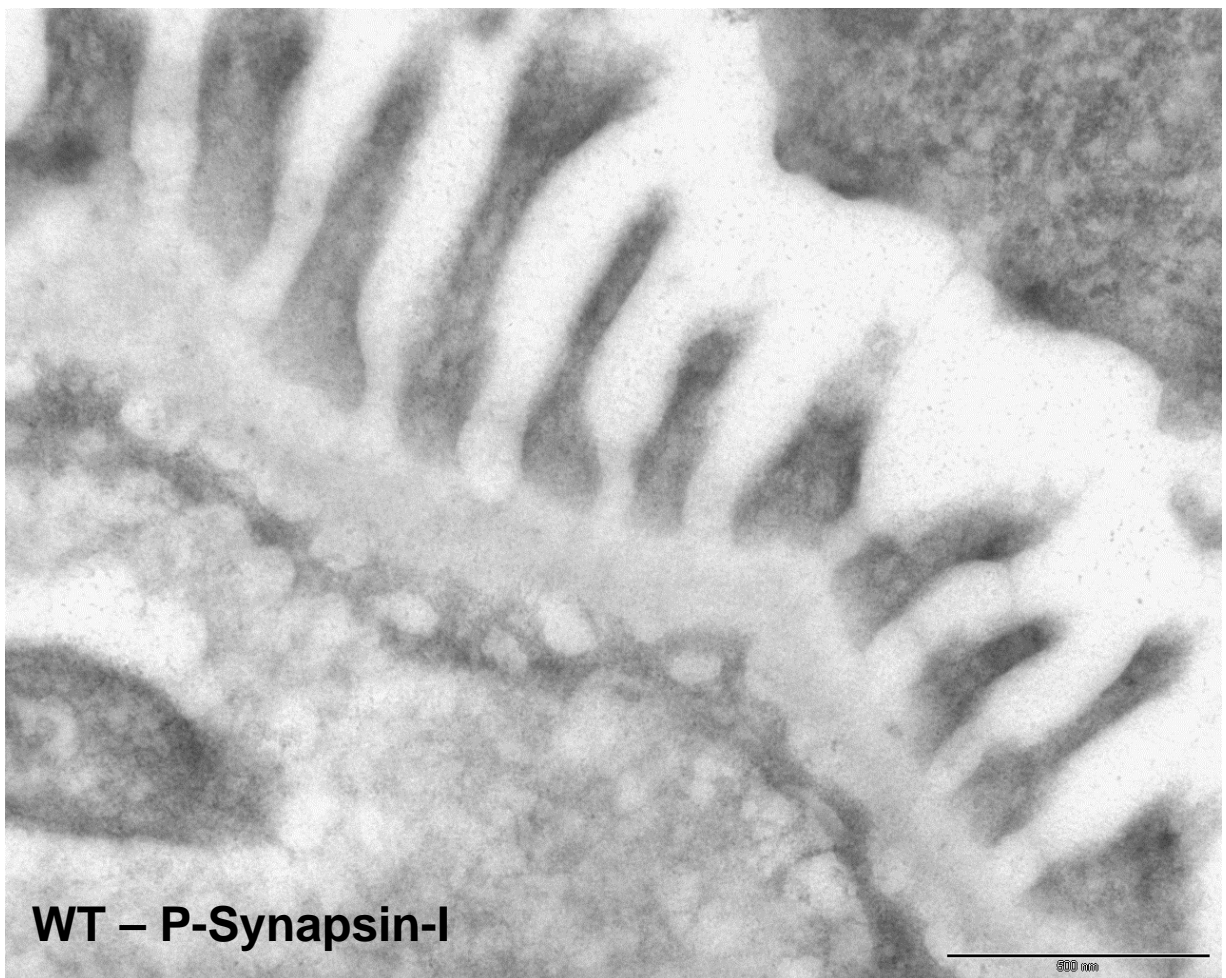
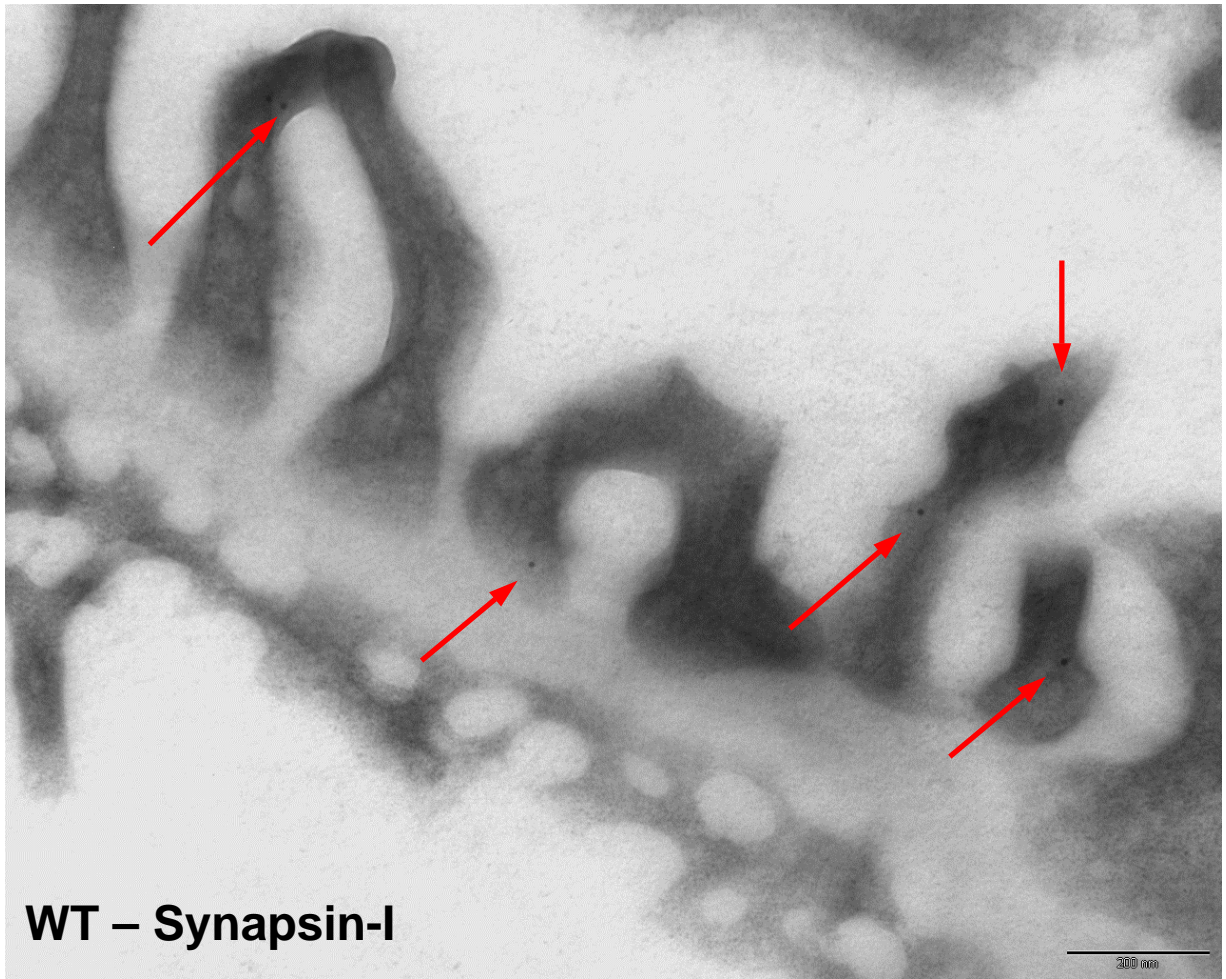
Suppl.Fig 4E



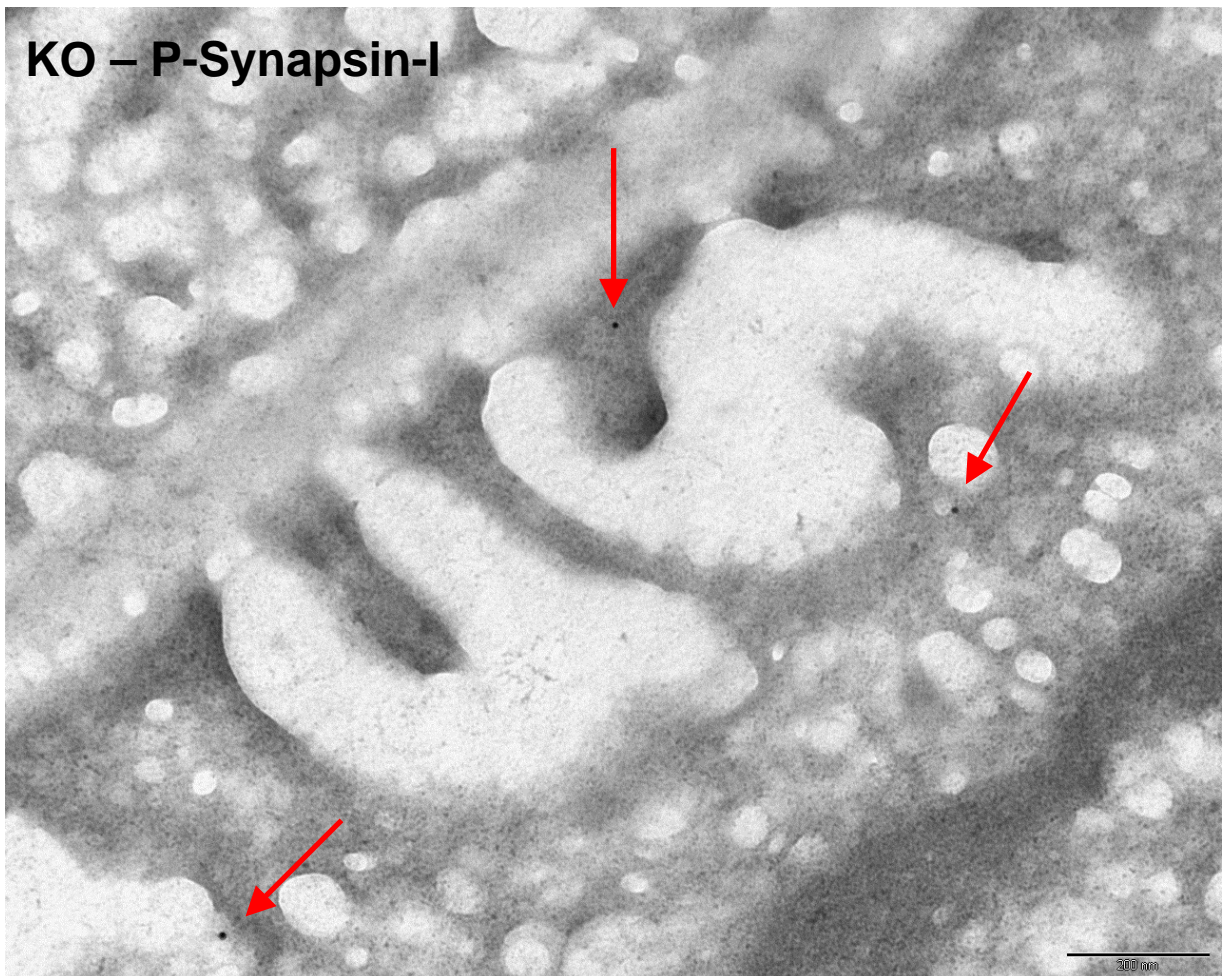
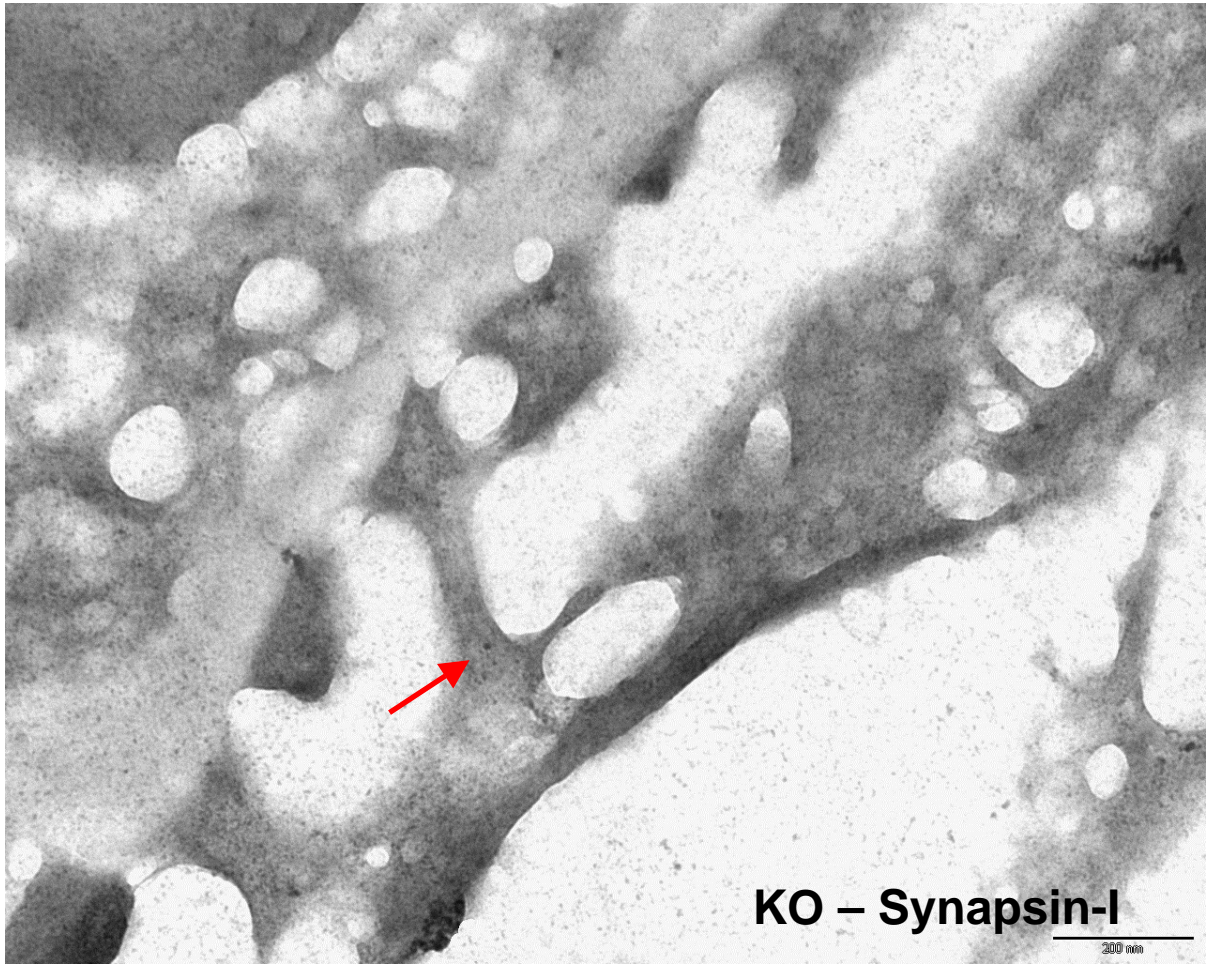
Suppl.Fig 4F



Suppl. Fig. 4G



Suppl.Fig 5A



Suppl.Fig 5B